Probing the symmetric Higgs portal with di-Higgs boson production

Christoph Englert[1,*] and Joerg Jaeckel[2,†]

[1]*Scottish Universities Physics Alliance, School of Physics & Astronomy, University of Glasgow,
Glasgow G12 8QQ, United Kingdom*
[2]*Institut für Theoretische Physik, Universität Heidelberg,
Philosophenweg 16, 69120 Heidelberg, Germany*

A coupling of a scalar, charged under an unbroken global $U(1)$ symmetry, to the Standard Model via the Higgs portal is one of the simplest gateways to a dark sector. Yet, for masses $m_S \geq m_H/2$ there are few probes of such an interaction. In this note, we evaluate the sensitivity to the Higgs portal coupling of di-Higgs boson production at the LHC as well as at a future high-energy hadron collider, FCC-hh, taking into account the full momentum dependence of the process. This significantly impacts the sensitivity compared to estimates of changes in the Higgs coupling based on the effective potential. We also compare our findings to precision single Higgs-boson probes such as the cross section for vector-boson-associated Higgs production at a future lepton collider, e.g., FCC-ee, as well as searches for missing energy-based signatures.

I. INTRODUCTION

Searches for a dark sector are often benchmarked by the use of three portals coupling particles neutral under the Standard Model (SM) gauge group to SM particles: the vector portal, the neutrino portal, and the Higgs portal [1–5]. On closer inspection, most investigations (see, e.g., the recent Ref. [6]) actually focus on the respective mixing effects—i.e., kinetic mixing between a new vector and the SM $U(1)$, neutrino mixing with a new neutral lepton, and mixing of the Higgs boson with a dark counterpart. However, in the case of the Higgs portal, there is the possibility to have an unbroken $U(1)$ or $\mathbb{Z}_2$ symmetry that forbids mixing effects. Although there are notable exceptions (cf., e.g., Refs. [7–9] for overviews), this case is much less explored and constrained. This is despite the fact that such a dark scalar could be a dark matter candidate both from thermal [9–16] and from nonthermal [17–19] production, and could also play a role in baryogenesis [7,20–23].

Let us consider the following simple Lagrangian for a dark scalar with an unbroken $\mathbb{Z}_2$ symmetry:

$$\mathcal{L} = \frac{1}{2}(\partial_\mu S)^2 - \frac{m_S^2}{2}S^2 - \lambda S^2(\Phi^\dagger\Phi - v^2/2), \qquad (1)$$

where λ specifies the Higgs portal coupling with the SM Higgs doublet Φ.

Experimental searches without the dark matter assumption are complicated by the fact that such a dark scalar can only be pair-produced via the exchange of at least one Higgs. In particular, for dark scalar mass above the threshold $m_H/2$, where the Higgs boson cannot decay into two scalars, sensitivity is severely limited.

In this note, we evaluate the impact of the virtual effects of such a dark scalar on Higgs boson pair production. While the LHC has relatively limited sensitivity, a future 100 TeV proton collider such as the so-called future circular hadron-hadron collider (FCC-hh) can viably test the unexplored parameter space for masses $m_S \leq m_H/2 \leq$ few $\times$ 100 GeV given the enhanced search potential of Higgs pair final states, e.g., Ref. [24]. Compared to earlier studies [7,21], we take into account the full, momentum-dependent one-loop amplitude (similar to what is done in Ref. [25] for a different dark matter model interacting with the Higgs boson, as well as Ref. [26], which considers a Higgs portal model in the nonmixing limit, but one without a $\mathbb{Z}_2$ symmetry) instead of considering the correction of the Higgs boson self-coupling obtained from the effective Coleman-Weinberg potential [27]. In particular, at low masses the threshold effects have significant impact, unfortunately somewhat reducing the actual sensitivity for some masses.

II. LIGHT SCALAR CONTRIBUTION TO HIGGS PAIR PRODUCTION

Let us start by explicitly writing down the portal interaction in terms of the Higgs, H, and the Goldstone modes, $\phi^\pm, \phi^0$. Writing the Higgs doublet as
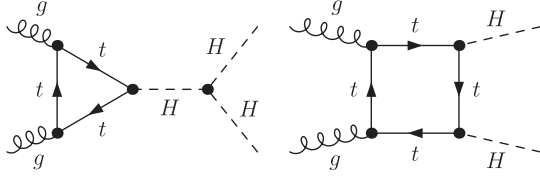
FIG. 1. Representative leading-order Feynman topologies contributing to $gg \to HH$ production.

$$\Phi = \frac{1}{\sqrt{2}} \begin{pmatrix} \sqrt{2}\phi_+ \\ v + H + i\phi_0 \end{pmatrix}, \tag{2}$$

we have

$$-\mathcal{L}_{\text{portal}} = \lambda \Phi^\dagger \Phi S^2 = +\frac{\lambda v^2}{2} S^2 + \lambda v H S^2 + \frac{\lambda}{2} H^2 S^2$$
$$+ \frac{\lambda}{2} \phi_0^2 S^2 + \lambda \phi_+ \phi_- S^2. \tag{3}$$

Note that with the above definitions, we denote the S particle's pole mass with m_S. The leading-order contributions to $gg \to HH$ are given by the Feynman topologies shown in Fig. 1. At the same time, relevant one-loop S contributions to the gluon fusion amplitude (modulo field renormalization constants) are due to the off-shell Higgs three-point function shown in Fig. 2.

Let $\mathcal{S}$ be the s-channel and $\mathcal{B}$ the box part of the one-loop $gg \to HH$ amplitude; i.e., the left- and right-hand sides of Fig. 1 where all possible fermion flow orientations are understood implicitly. The full $gg \to HH$ matrix element is then represented by

$$\mathcal{M} = \mathcal{S} + \mathcal{B}. \tag{4}$$

In the following, we will consider the one-loop S insertion for $\mathcal{S}$. Writing

$$\mathcal{S} = \mathcal{T} \frac{1}{s - m_H^2} \Gamma(s, m_H^2, m_H^2), \tag{5}$$

where $\mathcal{T}$ denotes the well-known expression of one-loop Higgs boson production [28,29], with $s = m_{HH}^2 = (p_{H,1} + p_{H,2})^2$, we can directly identify the leading-order (or Born-level) contribution,

$$\Gamma^{\text{Born}}(s, m_H^2, m_H^2) = -\frac{3m_H^2}{v} = -6\lambda_H^{\text{SM}}, \tag{6}$$

as the Higgs trilinear vertex in the SM. The virtual corrections induced by S arise from the diagrams depicted in Fig. 2 and are found to be

$$\Gamma^{\text{virt}}(s, m_H^2, m_H^2)$$
$$= \frac{\lambda}{16\pi^2 v} \left(\frac{3m_H^2 A_0(m_S^2)}{s - m_H^2} + 2\lambda v^2 \left\{ 2B_0(m_H^2, m_S^2, m_S^2) \right. \right.$$
$$+ 4\lambda v^2 C_0(m_H^2, m_H^2, s, m_S^2, m_S^2, m_S^2)$$
$$\left. \left. + B_0(s, m_S^2, m_S^2) \left[1 + \frac{3m_H^2}{s - m_H^2} \right] \right\} \right). \tag{7}$$

This contains divergences that are renormalized by the counterterm contributions shown in Fig. 3. In Eq. (7), A_0, B_0, and C_0 are the well-known one-loop Passarino-Veltman [30] functions in the convention of Refs. [31–34].
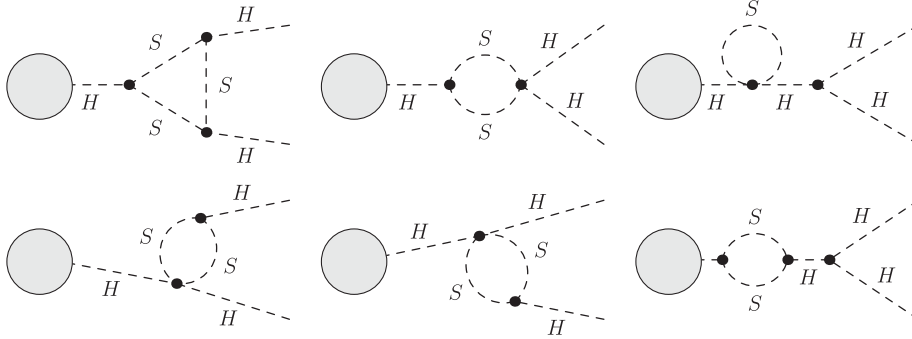

FIG. 2. One-loop contribution to s-channel $gg \to HH$ production. The shaded area represents the remainder (one-loop top insertion part) of the amplitude.
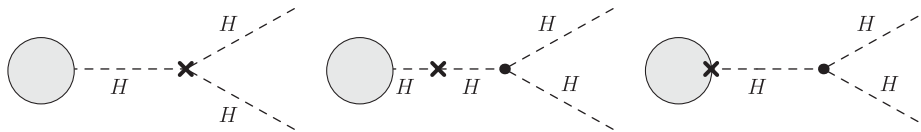

FIG. 3. Counterterm contribution to s-channel $gg \to HH$ production. The shaded area represents the remainder of the amplitude as in Fig. 2.

Tadpoles deserve a special comment, as they generate a nonvanishing contribution for the Higgs boson self-interaction renormalization (see, e.g., Ref. [31]). The SM Higgs potential reads, after inserting Eq. (2),

$$V_{\rm SM}(\Phi) = -\mu^2|\Phi|^2 + \lambda_H^{\rm SM}|\Phi|^4$$
$$\supset v(-\mu^2 + v^2\lambda_H^{\rm SM})H = tH. \qquad (8)$$

Here $t = v(-\mu^2 + v^2\lambda_H)$ vanishes at leading order due to the choice of v. Keeping track of $t = v(-\mu^2 + v^2\lambda_H)$ gives rise to a trilinear contribution,

$$V_{\rm SM}(\Phi) \supset \left(\frac{m_H^2}{2v} - \frac{t}{2v^2}\right)H^3. \qquad (9)$$

Our S-induced tadpole contributions can be removed through a choice that can be diagrammatically expressed as

$$\delta t + t = \delta t + \;\cdots\!\!-\!\!\bullet\!\!\bigcirc\; = 0, \qquad (10)$$

which amounts to performing the calculation with the "correct choice" of v. This allows us to neglect tadpole diagrams, as they would identically cancel against the associated counterterms. δt is straightforward to compute in our scenario,

$$\delta t = -\frac{\lambda v}{16\pi^2}\,\mathrm{Re}\,A_0(m_S^2), \qquad (11)$$

and needs to be considered in the renormalization of the three-point vertex function according to Eq. (9). The counterterm contribution is then given by

$$\Gamma^{\rm CT}(s, m_H^2, m_H^2) = -\frac{3}{v}\left(\frac{\delta t}{v} - \frac{\delta m_H^2 s}{s - m_H^2} - \frac{\delta Z_H m_H^2}{2}\right), \qquad (12)$$

where δZ_H and δm_H^2 are the Higgs wave function and mass renormalization constants. We use the on-shell renormalization scheme, where these parameters are given by

$$\delta Z_H = -\frac{\lambda^2 v^2}{8\pi^2}\frac{\partial}{\partial q^2}\,\mathrm{Re}\,B_0(q^2, m_S^2, m_S^2)|_{q^2=m_H^2} \qquad (13)$$

and

$$\delta m_H^2 = \frac{\lambda}{16\pi^2}\,\mathrm{Re}\,A_0(m_S^2) + \frac{\lambda^2 v^2}{8\pi^2}\,\mathrm{Re}\,B_0(m_H^2, m_S^2, m_S^2), \qquad (14)$$

respectively. In dimensional regularization with dimension $D < 4$, we can extract the divergent contributions for $D \to 4$ via

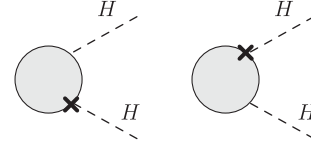$$A_0 = \frac{2m^2}{4-D} + \mathcal{O}([4-D]^0), \quad B_0 = \frac{2}{4-D} + \mathcal{O}([4-D]^0) \qquad (15)$$

FIG. 4. Counterterm contribution to the box graphs of $gg \to HH$ production. The shaded area represents the remainder (one-loop top insertion part) of the box amplitude.

to realize that

$$\Gamma^{\rm virt} + \Gamma^{\rm CT} = \mathcal{O}([4-D]^0) \qquad (16)$$

is manifestly UV-finite. δZ_H contains no UV singularity. The full renormalized s-channel amplitude is then (see also Ref. [26])

$$\mathcal{S}_{\rm virt} = \frac{\mathcal{T}}{s - m_H^2}\left(\Gamma^{\rm virt} + \Gamma^{\rm CT} + \frac{\delta Z_H}{2}\Gamma^{\rm Born}\right), \qquad (17)$$

where the last term stems from the counterterm contribution to the Higgs coupling as part of $\mathcal{T}$. The box contribution follows analogously (see Fig. 4):

$$\mathcal{B}_{\rm virt} = \delta Z_H \mathcal{B}_{\rm Born}. \qquad (18)$$

We obtain the full amplitude by expanding to $\mathcal{O}(\lambda^2)$:

$$|\mathcal{A}|^2 = |\mathcal{M}_{\rm Born}|^2 + 2\mathrm{Re}(\mathcal{M}_{\rm Born}\mathcal{M}_{\rm virt}^*). \qquad (19)$$

As $\mathcal{M}_{\rm virt}$ is UV-finite, we can include the $\mathcal{O}(\lambda^4)$ term $|\mathcal{M}_{\rm virt}|^2$ for comparison to gauge the importance of (factorizable) two-loop contributions, in particular when we consider numerically large couplings λ in our scan.

Through the choice of model, we implicitly assume that the dominant electroweak corrections indeed arise through the dynamics of S, and we will neglect the SM electroweak corrections, which are currently unknown, throughout. However, in direct relation to the SM expectation—i.e., when ratios are considered—the SM corrections will cancel at one-loop order. We have implemented the above calculation in a modified version of VBFNLO [35–38] that links the FEYNARTS/FORMCALC/LOOPTOOLS [32–34] to obtain numerical results.

III. RESULTS

Let us start by discussing the main features of di-Higgs production. The effect of the new scalars is mainly encoded in the modification of the three-point function. A comparison to the Standard Model value is shown in Fig. 5.[1] For relatively low masses of the new scalar, this exhibits a considerable momentum dependence as well as featuring a

---

[1]Although the quantity shown in Fig. 5 is not an observable, it is instructive to understand where corrections can be expected in physical quantities derived from Γ.
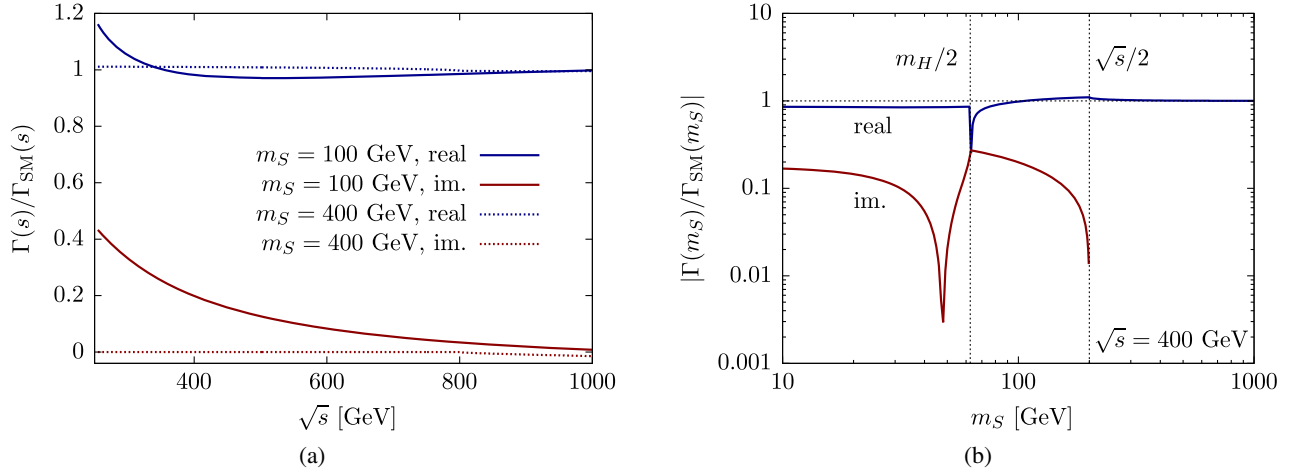
FIG. 5. (a) Comparison of the imaginary and the real parts of the three-point function Γ for ($\lambda = 1$) relative to SM ($\lambda = 0$) as a function of the invariant di-Higgs mass $\sqrt{s} = m_{HH}$. The turn-on of absorptive parts is visible for $m_S = 400$ GeV at $\sqrt{s} = m_{HH} = 2m_S = 800$ GeV. (b) The *modulus* of the three-point function relative to the SM as a function of m_S (again for $\lambda = 1$) for fixed $\sqrt{s} = 400$ GeV, which only allows us to resolve thresholds for up to $\sqrt{s}/2$.

real and an imaginary part. Both properties distinguish the full calculation from estimates based on a modified three-Higgs boson coupling obtained from the (explicitly momentum-independent) Coleman-Weinberg effective potential [7,21]. From Fig. 5, it also becomes clear that we quickly probe the decoupling limit for larger values of m_S (consistent with the expectation of Ref. [39]).

The price to pay for using a loop process is that it is higher order in the portal coupling λ. In practice, we find that sensitivity is limited to $\lambda \sim 1$, where these effects are accordingly non-negligible. At the same time, this raises the question of even higher-order corrections. As already mentioned in the previous section, we can use the $\mathcal{O}(\lambda^4)$ term $|\mathcal{M}_{\text{virt}}|^2$ to obtain some estimate of higher-order corrections beyond the $\mathcal{O}(\lambda^3)$ we have fully included. A comparison is shown in Fig. 6, giving us reasonable confidence in the calculations for couplings up to $\lambda \sim 1$, especially for light scalar masses.
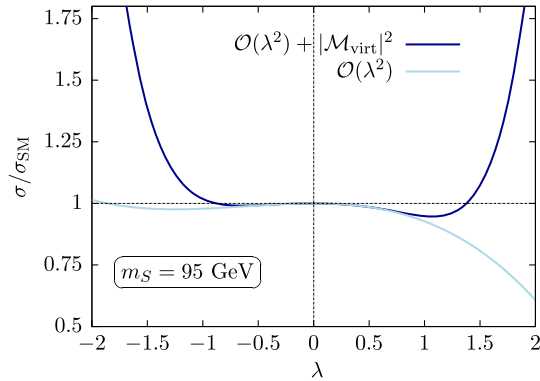
Let us now turn to the actual evaluation of the sensitivity. Most projections for the precision of di-Higgs rate measurements are quantified as sensitivities to changes in the Higgs boson self-coupling (cf., e.g., Refs. [24,40]). To make use of these, we compare the impact of virtual portal scalars against that of a (momentum-independent) change in the self-coupling as shown in Fig. 7. If the binned distribution deviates by more than the band indicated by the self-coupling projection in the sense of a binned χ^2 test, we consider a particular (m_S, λ) point to be excludable.

We consider the sensitivity both at the LHC and also at a future FCC. The implicit momentum dependence of $pp \to HH$ has been used to set constraints on the Higgs boson self-coupling by exploiting the destructive interference between the triangle and box contributions of Fig. 1. Given the relatively small cross section of HH production at the LHC of about 32 fb [41–49], the expected precision of the self-coupling extraction is going to be limited.

FIG. 6. Comparison of the cross section as a function of λ for different approximations, $m_S = 95$ GeV and $\sqrt{s} = 100$ TeV; for details, see text.
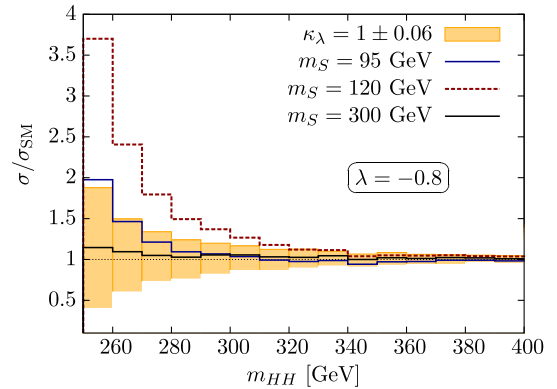

FIG. 7. Invariant di-Higgs mass spectra relative to the SM and 6% self-coupling extraction as described in Ref. [24].
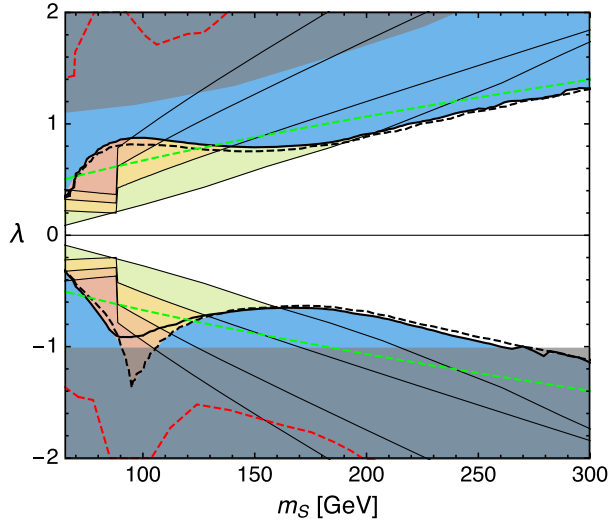
FIG. 8. Sensitivity projections for the di-Higgs boson production as well as other approaches. LHC di-Higgs results are shown as the red dashed line. For FCC-hh (100 TeV, 30/ab), we show as the solid (dashed) line the sensitivities obtainable from di-Higgs boson production based on a calculation without (with) terms $\sim |\mathcal{M}_{\mathrm{virt}}|^2$. The blue region shows the intersection of these two calculations and is in this sense conservative. The green dashed line shows the sensitivity expected from a simple effective potential approximation for the self-coupling [7,21]. The red, orange, and yellow regions correspond to the 1.7%, 1.06%, and 0.5% measurements [50] of the cross section of vector-boson-associated Higgs boson production at the future ILC-250 (International Linear Collider at 250 GeV), CLIC-380 (Compact Linear Collider at 380 GeV) and FCC-ee (electron-positron option of the FCC at 240 GeV), respectively. Finally, the light-green region indicates the best sensitivity curve from missing energy searches according to Ref. [8]. Regions where the electroweak vacuum is potentially endangered, obtained in Ref. [7], are shown in gray.

A recent projection by CMS [40] suggests that a sensitivity to $\lambda^{95\%\mathrm{CL}}_{\mathrm{SM}}/\lambda_{\mathrm{SM}} = [-0.18, 3.6]$ can be achieved, which corresponds to a gluon fusion cross section extraction of $\mathcal{O}(15\%)$ when assuming SM dynamics. The obtainable sensitivity is shown as the red dashed line in Fig. 8. As we can see, detectable effects typically require couplings λ significantly larger than 1, where our calculations are not fully trustworthy. To be conservative, we perform the calculation both with and without the squared virtual corrections and only show whatever sensitivity is weaker. However, it should be kept in mind that this still includes only part of the higher-order corrections, and therefore is only an estimate.

Di-Higgs boson production is one of the key motivators for pushing the high-energy frontier beyond the high-luminosity and high-energy LHC options. As shown in Ref. [24] (see also Refs. [51–57]), a coupling extraction of λ_{SM} at the $\lesssim 6\%$ level could be attainable at an FCC-hh with 100 TeV collisions and a 30/ab dataset. This is a direct

reflection of a much larger di-Higgs inclusive cross section of around 1 pb [47]. On the basis of this extrapolation, a much better sensitivity to the portal coupling can be achieved. This is shown as the solid black line and the blue region in Fig. 8, which now penetrates into the region $\lambda \lesssim 1$. To estimate the sensitivity to higher-order corrections, we show the dashed line that includes the squared virtual corrections.

The impact of the full calculation can be appreciated by comparison with the green dashed line, which is obtained from estimating the change in the Higgs' self-coupling by including the effects of the portal scalars in the Coleman-Weinberg effective potential as in Refs. [7,21].[2] The alert reader might realize that, for larger values of m_S, the full computation results in a systematically higher sensitivity than the effective potential calculation, where we could expect the Coleman-Weinberg approximation to be a good one according to Fig. 5. The reason for this difference is that the expected precision as given by the $\lambda_H/\lambda_H^{\mathrm{SM}} \sim \mathcal{O}(6\%)$ interpretation pushes us into a regime where weak corrections become relevant. These are not fully reflected by *ad hoc* rescalings of the Higgs boson self-coupling. Tree-level modifications $\lambda_H/\lambda_H^{\mathrm{SM}}$ are visible through threshold effects [58–61] (see also Ref. [52]). Effects of this type need to be contrasted with coherent Higgs boson coupling changes [62,63] that drive the destructive interference between the diagrams in Fig. 1—in particular, they affect the box diagrams. As the latter contributions are relevant even in the high-m_{HH} region where FCC-hh has significant sensitivity, there is an additional source of deviation compared to $\lambda_H/\lambda_H^{\mathrm{SM}}$ alone. The eventual sensitivity yield will obviously depend on the details of the machine itself as well as the status of SM precision calculations at the time. That said, it is clear that sufficiently large statistics could enable us to go beyond just finding a deviation from the SM and fingerprint the origin of the changes in the invariant di-Higgs boson mass spectrum (see also the recent Ref. [64]). As can be seen from Fig. 7, the dependence on the invariant mass for the portal scalar is quite different from a simple change in the Higgs boson self-coupling, allowing us to get information on the new physics giving rise to the deviation from the SM.

The sensitivity of di-Higgs boson production has to be appraised in the context of other approaches that have been suggested to constrain the model of Eq. (1). In the following, we concentrate on two main methods: the change in the cross section of vector-boson-associated Higgs boson production (Higgs-strahlung) [62,63,65]

---

[2]The Coleman-Weinberg effective potential [27] is given by $V(H) = -(\mu^2/2)H^2 + (\lambda_H/4)H^4 + (1/(64\pi^2))M^4(\mathrm{const.} + \log(M^2))$, where in our case $M^2 = m_S^2 + \lambda(H^2 - v^2)$. As in Ref. [21], we have fixed μ^2 and λ_H by implementing the condition that $v = 246$ GeV and $m_H^2 = (125 \text{ GeV})^2$. The results agree well with those of Ref. [7].

(see also Ref. [7]), and processes where the new scalars S are produced via an off-shell Higgs, typically leading to missing energy [8,9].

It is known that the associated weak corrections will modify the single Higgs boson production phenomenology [62,63,65], leading to measurable deviations in particular at future precision machines such as a future lepton collider, FCC-ee, in Z-boson-associated Higgs production. These constraints also do not depend on the energy momentum transfer, because the measurement will be focused on a very narrow energy range of around 240 GeV [66–69], where Z-boson-associated Higgs production is maximized. The energy spectrum of the incident electrons is typically sharp (see, e.g., Ref. [70]) for regions where $e^+e^- \rightarrow ZH$ production is relevant. The yellow region in Fig. 8 shows the sensitivity obtainable with an 0.5% [68] precision measurement of the cross section. We have performed similar analysis for the ILC-250 (1.06%) [50] and CLIC-380 (1.7%) [50], which are shown in orange and red, respectively.

At hadron colliders, the Higgs portal interaction leads to pair production of the new scalar S via an off-shell Higgs boson, giving rise to a missing energy signature [8,9]. Such analyses are difficult, as no resonance structure is available to control backgrounds. In parallel, the cross section has a steep dropoff as a function of the Higgs bosons' virtuality due to the propagator suppression. However, we can expect considerable sensitivity, in particular when we turn to 100 TeV collisions with large statistics 30/ab [8], which are given by the light-green region in Fig. 8. Another possibility at hadron colliders is off-shell Higgs boson production in Z-pair final states. The nondecoupling of the Higgs contribution due to unitarity arguments [71] has been used to set constraints on the Higgs boson width [72] under certain assumptions [73,74]. It has been shown that a fair part of corrections cancel in this channel [75], and an explicit calculation shows that only subpercent modifications of the Higgs signal in ZZ can be expected in the region selected by the HH production projection. This small modification needs to be contrasted with a dominant $gg \rightarrow ZZ$ continuum, which makes HH production the more relevant channel in the light of the associated three-point modification that is magnified by the interference effects in the HH threshold region.

Finally, we also remark that a viable electroweak symmetry breaking vacuum is endangered if the portal coupling is too large [7]. We indicate the region where nonperturbatively large self-couplings of the scalar S are needed to avoid this fate according to Ref. [7] as the gray region. This shows that the LHC's sensitivity in HH production is not large enough to test a viable region of the model's parameter space in this channel.

IV. SUMMARY AND CONCLUSIONS

Higgs physics remains an exciting avenue to explore the potential presence of new interactions beyond the Standard Model. In particular, given the gauge-singlet nature of the $|\Phi|^2$ operator, a fully renormalizable scalar (Higgs portal) extension $\sim |\Phi|^2 S^2$ of the SM is a motivated possibility. While such models can be efficiently constrained when the additional scalar obtains a vacuum expectation value [76–79] or is light enough for the decay $H \rightarrow SS$ to be open (cf., e.g., Refs. [9,80] for a recent discussion), once $m_S > m_H/2$, the sensitivity becomes limited directly as a consequence of the (weak) Higgs-related production. At hadron colliders, off-shell Higgs boson measurements can provide direct sensitivity [8] that is limited ultimately by the reduction of the cross section for masses too far away from the Higgs resonance. In these circumstances—i.e., when the probed center-of-mass energy is high enough— these scalars can manifest themselves as virtual contributions through (but not limited to) absorptive parts of the amplitude. This motivates the precision study of double Higgs boson final states (see also Ref. [25]) as an indirect probe, which is expected to become a sensitive probe of electroweak physics at a future high-energy proton collider. In this work, we have shown that the expected precision of the Higgs self-coupling extraction at a 100 TeV FCC-hh [24] indeed shows competitive (yet model-dependent) sensitivity to this scenario, with complementarity to precision studies of Higgs-strahlung processes at, e.g., lepton colliders [63,65]. This shows that the energy coverage and the large anticipated dataset at such a machine can provide a competitive electroweak precision physics instrument (see also Refs. [81,82]).

[1] T. Binoth and J. J. van der Bij, Z. Phys. C **75**, 17 (1997).
[2] R. M. Schabinger and J. D. Wells, Phys. Rev. D **72**, 093007 (2005).
[3] B. Patt and F. Wilczek, arXiv:hep-ph/0605188.
[4] M. Ahlers, J. Jaeckel, J. Redondo, and A. Ringwald, Phys. Rev. D **78**, 075005 (2008).
[5] B. Batell, M. Pospelov, and A. Ritz, Phys. Rev. D **79**, 115008 (2009).
[6] J. Beacham et al., arXiv:1901.09966.
[7] D. Curtin, P. Meade, and C.-T. Yu, J. High Energy Phys. 11 (2014) 127.
[8] N. Craig, H. K. Lou, M. McCullough, and A. Thalapillil, J. High Energy Phys. 02 (2016) 127.
[9] G. Arcadi, A. Djouadi, and M. Raidal, arXiv:1903.03616.
[10] V. Silveira and A. Zee, Phys. Lett. **161B**, 136 (1985).
[11] J. McDonald, Phys. Rev. Lett. **88**, 091304 (2002).
[12] H. Davoudiasl, R. Kitano, T. Li, and H. Murayama, Phys. Lett. B **609**, 117 (2005).
[13] V. Barger, P. Langacker, M. McCaskey, M. J. Ramsey-Musolf, and G. Shaughnessy, Phys. Rev. D **77**, 035005 (2008).
[14] V. V. Khoze, C. McCabe, and G. Ro, J. High Energy Phys. 08 (2014) 026.
[15] L. Feng, S. Profumo, and L. Ubaldi, J. High Energy Phys. 03 (2015) 045.
[16] P. Athron, J. M. Cornell, F. Kahlhoefer, J. Mckay, P. Scott, and S. Wild, Eur. Phys. J. C **78**, 830 (2018).
[17] E. Hardy, J. High Energy Phys. 06 (2018) 043.
[18] N. Bernal, C. Cosme, T. Tenkanen, and V. Vaskonen, Eur. Phys. J. C **79**, 30 (2019).
[19] G. Alonso-Álvarez, J. Gehrlein, J. Jaeckel, and S. Schenk, J. Cosmol. Astropart. Phys. 09 (2019) 003.
[20] J. R. Espinosa and M. Quiros, Phys. Rev. D **76**, 076004 (2007).
[21] A. Noble and M. Perelstein, Phys. Rev. D **78**, 063518 (2008).
[22] J. R. Espinosa, T. Konstandin, J. M. No, and M. Quiros, Phys. Rev. D **78**, 123528 (2008).
[23] J. R. Espinosa, T. Konstandin, and F. Riva, Nucl. Phys. **B854**, 592 (2012).
[24] R. Contino et al., CERN Yellow Report No. CERN-TH-2016-113, 2017, pp. 255–440.
[25] A. Voigt and S. Westhoff, J. High Energy Phys. 11 (2017) 009.
[26] S.-P. He and S.-h. Zhu, Phys. Lett. B **764**, 31 (2017).
[27] S. R. Coleman and E. J. Weinberg, Phys. Rev. D **7**, 1888 (1973).
[28] H. M. Georgi, S. L. Glashow, M. E. Machacek, and D. V. Nanopoulos, Phys. Rev. Lett. **40**, 692 (1978).
[29] S. Dawson, C. Englert, and T. Plehn, Phys. Rep. **816**, 1 (2019).
[30] G. Passarino and M. J. G. Veltman, Nucl. Phys. **B160**, 151 (1979).
[31] A. Denner, Fortschr. Phys. **41**, 307 (1993).
[32] T. Hahn and M. Perez-Victoria, Comput. Phys. Commun. **118**, 153 (1999).
[33] T. Hahn, Nucl. Phys. B, Proc. Suppl. **89**, 231 (2000).
[34] T. Hahn, Comput. Phys. Commun. **140**, 418 (2001).
[35] K. Arnold et al., Comput. Phys. Commun. **180**, 1661 (2009).
[36] J. Baglio et al., arXiv:1107.4038.
[37] K. Arnold et al., arXiv:1207.4975.
[38] J. Baglio et al., arXiv:1404.3940.
[39] T. Appelquist and J. Carazzone, Phys. Rev. D **11**, 2856 (1975).
[40] CMS Collaboration Prospects for HH measurements at the HL-LHC, CERN LHC Report No. CMS-PAS-FTR-18-019, 2018.
[41] R. Frederix, S. Frixione, V. Hirschi, F. Maltoni, O. Mattelaer, P. Torrielli, E. Vryonidou, and M. Zaro, Phys. Lett. B **732**, 142 (2014).
[42] D. de Florian and J. Mazzitelli, J. High Energy Phys. 09 (2015) 053.
[43] D. de Florian, M. Grazzini, C. Hanga, S. Kallweit, J. M. Lindert, P. Maierhöfer, J. Mazzitelli, and D. Rathlev, J. High Energy Phys. 09 (2016) 151.
[44] S. Borowka, N. Greiner, G. Heinrich, S. P. Jones, M. Kerner, J. Schlenk, U. Schubert, and T. Zirke, Phys. Rev. Lett. **117**, 012001 (2016); **117**, 079901(E) (2016).
[45] S. Borowka, N. Greiner, G. Heinrich, S. P. Jones, M. Kerner, J. Schlenk, and T. Zirke, J. High Energy Phys. 10 (2016) 107.
[46] G. Heinrich, S. P. Jones, M. Kerner, G. Luisoni, and E. Vryonidou, J. High Energy Phys. 08 (2017) 088.
[47] M. Grazzini, G. Heinrich, S. Jones, S. Kallweit, M. Kerner, J. M. Lindert, and J. Mazzitelli, J. High Energy Phys. 05 (2018) 059.
[48] D. De Florian and J. Mazzitelli, J. High Energy Phys. 08 (2018) 156.
[49] J. Baglio, F. Campanario, S. Glaus, M. Mühlleitner, M. Spira, and J. Streicher, Eur. Phys. J. C **79**, 459 (2019).
[50] J. de Blas et al., arXiv:1905.03764.
[51] W. Yao, in Proceedings, 2013 Community Summer Study on the Future of U.S. Particle Physics: Snowmass on the Mississippi (CSS2013): Minneapolis, MN, USA (2013), http://www.slac.stanford.edu/econf/C1307292/docs/submittedArxivFiles/1308.6302.pdf.
[52] A. J. Barr, M. J. Dolan, C. Englert, D. E. Ferreira de Lima, and M. Spannowsky, J. High Energy Phys. 02 (2015) 016.
[53] H.-J. He, J. Ren, and W. Yao, Phys. Rev. D **93**, 015003 (2016).
[54] A. Papaefstathiou, Phys. Rev. D **91**, 113016 (2015).
[55] A. Adhikary, S. Banerjee, R. K. Barman, B. Bhattacherjee, and S. Niyogi, J. High Energy Phys. 07 (2018) 116.
[56] S. Banerjee, C. Englert, M. L. Mangano, M. Selvaggi, and M. Spannowsky, Eur. Phys. J. C **78**, 322 (2018).
[57] S. Banerjee, F. Krauss, and M. Spannowsky, Phys. Rev. D **100**, 073012 (2019).
[58] E. W. N. Glover and J. J. van der Bij, Nucl. Phys. **B309**, 282 (1988).
[59] U. Baur, T. Plehn, and D. L. Rainwater, Phys. Rev. Lett. **89**, 151801 (2002).
[60] U. Baur, T. Plehn, and D. L. Rainwater, Phys. Rev. D **67**, 033003 (2003).
[61] U. Baur, T. Plehn, and D. L. Rainwater, Phys. Rev. D **68**, 033001 (2003).
[62] C. Englert and M. McCullough, J. High Energy Phys. 07 (2013) 168.
[63] N. Craig, C. Englert, and M. McCullough, Phys. Rev. Lett. **111**, 121803 (2013).

[64] M. Capozi and G. Heinrich, arXiv:1908.08923.

[65] N. Craig, M. Farina, M. McCullough, and M. Perelstein, J. High Energy Phys. 03 (2015) 146.

[66] M. E. Peskin, arXiv:1207.2516.

[67] M. Bicer *et al.* (TLEP Design Study Working Group), J. High Energy Phys. 01 (2014) 164.

[68] M. Klute, R. Lafaye, T. Plehn, M. Rauch, and D. Zerwas, Europhys. Lett. **101**, 51001 (2013).

[69] A. Abada *et al.* (FCC Collaboration), Eur. Phys. J. Spec. Top. **228**, 261 (2019).

[70] S. T. Boogert and D. J. Miller, Questions about the measurement of the e^+e^- luminosity spectrum at a future linear collider in *Linear Colliders. Proceedings, International Workshop on Physics and Experiments with Future Electron-Positron Linear Colliders, LCWS 2002, Seogwipo, Jeju Island, Korea* (2002), pp. 509–516.

[71] N. Kauer and G. Passarino, J. High Energy Phys. 08 (2012) 116.

[72] F. Caola and K. Melnikov, Phys. Rev. D **88**, 054024 (2013).

[73] C. Englert and M. Spannowsky, Phys. Rev. D **90**, 053003 (2014).

[74] C. Englert, Y. Soreq, and M. Spannowsky, J. High Energy Phys. 05 (2015) 145.

[75] C. Englert, G. F. Giudice, A. Greljo, and M. Mccullough, J. High Energy Phys. 09 (2019) 041.

[76] C. Englert, T. Plehn, D. Zerwas, and P. M. Zerwas, Phys. Lett. B **703**, 298 (2011).

[77] D. Bertolini and M. McCullough, J. High Energy Phys. 12 (2012) 118.

[78] C. Bernaciak, T. Plehn, P. Schichtel, and J. Tattersall, Phys. Rev. D **91**, 035024 (2015).

[79] T. Robens and T. Stefaniak, Eur. Phys. J. C **75**, 104 (2015).

[80] M. Cepeda *et al.* (HL/HE WG2 group), arXiv:1902.00134.

[81] R. Franceschini, G. Panico, A. Pomarol, F. Riva, and A. Wulzer, J. High Energy Phys. 02 (2018) 111.

[82] S. Banerjee, C. Englert, R. S. Gupta, and M. Spannowsky, Phys. Rev. D **98**, 095012 (2018).